

# Effective Field Theory Approach to Phase Transitions

Jens O. Andersen

Department of Physics, The Ohio State University, Columbus, OH 43210

## Abstract

In this paper I discuss the effective field theory approach, recently developed by Braaten and Nieto in the investigation of quantum field theories at high temperature. I demonstrate that this method can be easily extended to the study of phase transitions in theories with spontaneous symmetry breaking. The first step consists of the construction of a sequence of two effective three-dimensional field theories, which are valid on successively longer distance scales. The second step in the study of the phase transition is using the second effective Lagrangian in either perturbative calculations or lattice simulations. I apply the method to a theory which consists of  $N$  charged  $U(N)$  symmetric scalars coupled to an Abelian gauge field. The effective Lagrangian can then be used on the lattice to investigate the order of the phase transition as a function of  $N$ .

PACS number(s): 11.10.Wx, 12.20.Ds, 12.38.Bx

# 1 Introduction

Many problems in quantum field theory at high temperature have been studied extensively since the work of Dolan and Jackiw on symmetry restoration almost twenty five years ago [1]. There has also been tremendous progress in perturbative calculations and the methods available for the investigation of quantum systems at high temperature.

Today, there are essentially two ways of doing high temperature field theory. The first method is resummed perturbation theory, which mainly is due to Braaten and Pisarski [2] (See also Ref. [3] for an overview). Resummation is a reorganization of the ordinary perturbation expansion, which involves effective propagators and effective vertices. Naive perturbation theory breaks down for soft external momentum  $k$  ( $k \sim gT$ , where  $g$  is some generic coupling constant), due to infrared divergences. Leading order results for physical quantities, e.g. the gluon damping rate, get contributions from all orders in the loop expansion. The reorganization of perturbation theory provided by the resummation program is necessary in order to do consistent perturbative calculations at high temperature. The effective expansion sums up the infinite subset of infrared diagrams mentioned above, and it is truly perturbative in the sense that perturbative corrections are down by factors of  $g$ . Different resummation approaches have been used in perturbative studies of phase transitions in the Abelian Higgs model [4,5] and in the standard model [5,6]. Resummation has also been applied to calculate e.g. the free energy in  $g^2$ -theory [7,8], QED [9-11] and QCD [11-12].

The second method is that of effective field theory [13]. The general idea is to take advantage of two or more well separated mass scales in the problem by treating one scale at a time. This is done by constructing a sequence of effective field theories which are valid on successive longer distance scales and where the parameters of the effective Lagrangian encode the high energy physics [13]. In  $g^2$ -theory there are two mass scales. One scale is provided by the nonzero Matsubara frequencies of order  $2\pi nT$ , where  $n$  is a positive integer, and the other is given by the zero-frequency mode of order  $gT$  [14] (This mode acquires a thermal mass of order  $gT$  at one-loop order). In QCD, there are three momentum scales involved. These are the scale  $T$  arising from the nonzero Matsubara modes, and the scales  $gT$  and  $g^2T$  which are the scales of colour electric screening and colour magnetic screening, respectively [15]. Thus, it proves useful to construct a sequence of two effective field theories (called electrostatic and magnetostatic QCD) as demonstrated by Braaten and Nieto [17]. One advantage of using effective field theory instead of more conventional methods, is that one does not mix the different momentum scales in actual calculations, but treats them systematically one by one. This normally simplifies calculations considerably and is now a well established tool. Moreover, the capability of the effective field theory approach to isolate or separate the physics at different scales is very satisfactory from a physical point of view, since this gives better

insight into the system's one wishes to describe. Effective field theory has been used to calculate e.g. the free energy in QCD [16],  $g^2$ -theory [17] and QED [18]. The effective field theory approach has also been used in investigating the phase transition in the Abelian Higgs model [18,19], the standard model [21] as well as supersymmetric extensions [22].

There are also other advantages of the effective field theory approach that we wish to point out. In some cases it can solve problems, where other methods fail. A prominent example of this is the long-standing infrared catastrophe of QCD [23]. It is a well-known fact that the free energy of Non-Abelian gauge theories may be calculated to fifth order in the coupling using resummed perturbation theory. However, the method breaks down at order  $g^6$ , due to infrared divergences, as first pointed out by Linde [23]. These divergences arise from regions where all internal energies vanish, and so the singularities are the same as in three-dimensional pure QCD. Thus, the breakdown of perturbation theory simply reflects the infrared problems appearing in a perturbative treatment of any Non-Abelian gauge theory in three dimensions. In the effective field theory approach by Braaten and Nieto [16], one can compute order by order in the gauge coupling  $g$  the contributions to the free energy, although some coefficients must be evaluated numerically. The infrared problems can naturally be avoided if one uses lattice simulations directly in four dimensions. However, this is extremely time consuming in comparison with three-dimensional calculations and the time savings here arise from the reduction of the problem from four to three dimensions, and also by integrating out the fermions.

In recent years a combination of analytical and numerical methods has been used to study a number of problems in high temperature field theory. One very important subject is the investigation of the electroweak phase transition, which took place when the Universe was at a temperature of approximately 200 GeV. There is a variety of reasons for the interest in the electroweak phase transition. One of them is that the baryon asymmetry we observe today could be a remnant from the phase transition. For electroweak matter at a temperature around  $T_c$  there is a hierarchy of three momentum scales, and so again it is convenient to construct a sequence of two three-dimensional effective field theories. Normally, the perturbation expansion breaks down for temperatures close to  $T_c$ , so one must apply nonperturbative methods such as lattice simulations. Again it is more economical to use these three-dimensional field theories on the lattice than attacking the problem by brute force in four dimensions.

In the present work we would like to apply the method of Braaten and Nieto [16] in the constructing effective three-dimensional field theories which can be used in the study of phase transitions. The extension from previous applications is rather straightforward. More specifically, we apply the methods to a  $U(1)$  gauge theory coupled to  $N$  charged  $U(N)$  symmetric scalars. This is simply scalar electrodynamics where the scalar field is an  $N$ -component complex vector, and we shall refer to this model as SQED in the following.

This theory has previously been investigated by Arnold [24] and Lawrie [25] using the  $\epsilon$ -expansion. This method indicates that the order of the phase transition depends on the number of scalar fields  $N$ . Numerical study of the effective field theory obtained in the present paper, would give valuable information of the applicability of the  $\epsilon$ -expansion.

The plan of the article is as follows. In section II we discuss dimensional reduction and the hierarchy of momentum scales in quantum fields theories at finite temperature. We also discuss the construction of effective three-dimensional field theories. In section III and IV we determine the coefficients in the two effective field theories arising in our model. In section V we summarize and conclude. In Appendix A and B, the notation and conventions are given. We also list the sum-integrals in the full theory as well as the integrals in the effective theories which are needed in the present work. Appendix C provides the reader with a few examples of the calculations of the sum-integrals and the integrals which appear.

## 2 Dimensional Reduction and Effective Field Theories

Let us begin our discussion of dimensional reduction and effective field theories by considering  $g^2 = 4$ -theory. The Euclidean Lagrangian reads

$$L_E = \frac{1}{2} (\partial_\mu \phi)^2 + \frac{1}{2} m^2 \phi^2 + \frac{g^2}{24} \phi^4; \quad (1)$$

In the broken phase, we split the scalar field into a background field  $\phi_0$  and a quantum field  $\phi$  in the usual way

$$\phi = \phi_0 + \phi; \quad (2)$$

After this shift the tree-level mass of the scalar field is

$$m^2 = \frac{1}{2} m^2 + \frac{g^2}{6} \phi_0^2; \quad (3)$$

Let us now compute the one-loop correction to the two-point function. This is given by the tadpole diagram shown in Fig. 1. It is independent of the external momentum. The two-point function in the one-loop approximation then reads

$$(k_0; k) = k_0^2 + k^2 + m^2 + \frac{g^2}{2} \int \frac{1}{(p^2 + m^2)}; \quad (4)$$

Here,  $k = |k|$ . In the high temperature limit, where we ignore the tree-level mass in the propagator, it is straightforward to evaluate. One finds

$$(k_0; k) = k_0^2 + k^2 + m^2 + \frac{g^2}{24} T^2; \quad (5)$$

This implies that the field acquires an effective thermal mass

$$M^2 = m^2 + \frac{g^2 T^2}{24}; \quad (6)$$

Now, the scalar field theory undergoes a second order phase transition at  $T_c^2 = \frac{24}{g^2} m^2$  [4]. Moreover, for temperatures in the vicinity of  $T_c$ , the effective scalar mass is of order  $g^2 T$ , while for  $T \gg T_c$ , the effective scalar mass is of the order  $gT$  [21].

In the imaginary time formalism one can associate a propagator

$$D_n(k) = \frac{1}{\omega_n^2 + k^2}; \quad (7)$$

where  $\omega_n = 2\pi nT$  is the  $n$ th Matsubara frequency. This implies that one can view a four dimensional quantum field theory at finite temperature as a quantum field theory in three dimensions with infinitely many fields, and where the Matsubara frequencies act as tree level masses [14]. For the fields with nonzero Matsubara frequencies, the effective scalar mass  $M$  represents a perturbative correction, and these fields are still characterized by a mass of order  $T$ . However, the bosonic field with  $n = 0$ , is now characterized by a mass of order  $g^2 T$  or  $gT$  depending on temperature. In either case, as long as  $g^2 \gg 1$ , we have two widely separated mass scales. In analogy with the Appelquist-Carrazzone theorem at zero temperature [26], one expects that the nonzero Matsubara frequencies decouple at the scale  $gT$  (or  $g^2 T$ ) and that we can describe the system by an effective field theory of the zero-frequency mode of the scalar field. The resulting field theory is three-dimensional and the process of going from the full four-dimensional field theory to an effective field theory in three dimensions is called dimensional reduction [14].

In the original approach, mainly due to Ginsparg [27] and Landsman [14], one explicitly integrates out the nonzero Matsubara modes. The parameters in the effective Lagrangian is determined by considering the one-loop correction from the nonstatic modes to a static correlator. In other words, only nonzero modes circulate in the loop.

However, beyond the one-loop approximation this approach becomes more problematic. Integrating out the nonzero modes in the above meaning of the word, implies that one considers the effects of the nonstatic modes in the loops. However, higher order corrections to a static correlator also involve contributions where some of the Matsubara frequencies are zero while others are nonzero. Such contributions do not necessarily vanish, and one example of this is provided by the setting sun diagram in  $g^2 = 4$ -theory, where one Matsubara frequency is zero, while the two others are nonzero [21]. The neglect of such contributions results in non-local operators which cannot be expanded in local operators [28]. Hence, it is difficult to obtain a local effective Lagrangian.

This problem has been solved by the method proposed by Kajantie, Laine, Rummukainen and Shaposhnikov [21]. Here, the parameters are determined by a matching

requirement. One demands that static correlators in the full four-dimensional theory are reproduced to some accuracy by the correlators in the effective theory. In particular this approach allows for the simultaneous presence of static and nonstatic modes in multi-loop graphs (see also Ref. [29] for a thorough discussion of this in the case of  $g^2$  theory).

In many cases, one needs the static correlators at zero external momenta. This implies that one can use the effective potential directly, since this is the generator of connected Green's functions at vanishing external momenta. One advantage of the application of the effective potential is that it is often easier to calculate it as compared to the evaluation of loop corrections to some  $n$ -point function. A disadvantage is that one must explicitly distinguish between the contributions to a correlator from static and nonstatic modes.

There exists another approach to effective field theory, which does not explicitly distinguish between zero and nonzero Matsubara modes as in the methods outlined above. This approach is due to Braaten and Nieto [17]. One writes down the most general Lagrangian of the three-dimensional fields and which respects the symmetries of the system at finite temperature. Modern developments in renormalization theory guarantee that static correlators in the full theory can be reproduced by the effective theory at long distances  $R \gg 1/T$  by adding sufficiently many operators to the effective Lagrangian and tuning their coefficients as functions of the parameters in the full theory and temperature. The effective Lagrangian is nonrenormalizable and contains infinitely many operators. This method will be described in some detail below.

Let us next consider a  $U(1)$  gauge theory coupled to  $N$  charged  $U(N)$  symmetric scalars. The Euclidean Lagrangian for this theory reads

$$L_{\text{SQED}} = \frac{1}{4} F_{\mu\nu}^2 + (D_\mu \phi)^\dagger (D_\mu \phi) + \frac{1}{2} \partial_\mu \phi^\dagger \partial_\mu \phi + \frac{1}{6} (\phi^\dagger \phi)^2 + L_{\text{gf}} + L_{\text{gh}} \quad (8)$$

Here  $D_\mu = \partial_\mu + ieA_\mu$  is the covariant derivative and  $\phi = (\phi_1; \phi_2; \dots; \phi_N)$  is the corresponding column vector.

In the present work, we perform the calculations in the Landau gauge. This is merely a convenient choice, since many of the diagrams vanish in this gauge. The gauge fixing term is

$$L_{\text{gf}} = \frac{1}{2} (\partial_\mu A_\mu)^2; \quad \phi = 0 \quad (9)$$

If  $\phi$  denotes the ghost field, the ghost term reads

$$L_{\text{gh}} = (\partial_\mu \phi)^\dagger (\partial_\mu \phi) \quad (10)$$

Thus, the ghost term decouples from the rest of the Lagrangian. In the Landau gauge the scalar and vector propagators take the form

$$\langle \phi \phi \rangle = \frac{1}{p^2}; \quad \langle A_\mu A_\nu \rangle = \frac{p_\mu p_\nu - p^2 \delta_{\mu\nu}}{p^4} \quad (11)$$

After the shift in the Higgs field, the tree-level masses of the Higgs, Goldstone and the vector particle are, respectively

$$m_1^2 = \mu^2 + \frac{1}{2} g_0^2; \quad m_2^2 = \mu^2 + \frac{1}{6} g_0^2; \quad m_V^2 = e^2 g_0^2: \quad (12)$$

The Higgs field, the Goldstone field and the timelike component of the gauge field acquire effective thermal masses in analogy with the example above. In the next section, we shall demonstrate that thermal masses to leading order are

$$M_1^2 = m_1^2 + \frac{(N+1) T^2 + 9e^2 T^2}{36}; \quad (13)$$

$$M_2^2 = m_2^2 + \frac{(N+1) T^2 + 9e^2 T^2}{36}; \quad (14)$$

$$M_{A_0} = m_V^2 + \frac{e^2 T^2}{3}: \quad (15)$$

For  $T \gg T_c$ , the zero-frequency modes of the Higgs and Goldstone fields are characterized by masses of order  $e^2 T$ , while the temporal component of the gauge field has a mass of order  $eT$  (assuming that  $e^2 \ll 1$ ). This implies that for temperatures close to  $T_c$ , we have three different mass scales. For temperatures  $T \gg T_c$  the scalar field has a mass of the same order as the temporal component of the gauge field, and so there are only two mass scales. These observations suggest that we make a sequence of two effective field theories which are valid on successively longer distance scales.

Now that we have considered the different momentum scales in both  $g^2 \ll 1$ -theory and  $U(1)$  coupled to Higgs, we are ready to discuss the construction of the sequence of two effective three-dimensional field theories. The fields in the effective theories can approximately be identified with the zero-frequency modes of the original fields. The first effective field theory is called electrostatic Scalar electrodynamics (ESQED).  $L_{\text{ESQED}}$  consists of a real massive scalar field, which can be identified with the zero mode of the temporal component of the gauge field. We denote this field by  $\phi$ . Moreover, we have the  $N$ -component scalar field  $\Phi$  and the three-dimensional gauge field  $A_i^{3d}$  which are associated with the zero-frequency modes of  $A_0$  and  $A_i$  in SQED, respectively. The relations between the fields in SQED and ESQED are to a first approximation

$$\phi(\vec{x}) = \frac{1}{\sqrt{V}} \int d^3x' A_0(\vec{x}'); \quad A_i^{3d}(\vec{x}) = \frac{1}{\sqrt{V}} \int d^3x' A_i(\vec{x}'); \quad \Phi(\vec{x}) = \frac{1}{\sqrt{V}} \int d^3x' \Phi(\vec{x}'): \quad (16)$$

Beyond leading order, there are corrections to these equations, and we shall discuss this in subsection 3.1.

The symmetries are as follows: There is a gauged  $U(N)$  symmetry of  $\Phi$  and a rotational as well as a  $Z_2$ -symmetry of  $\phi$ . Moreover, the fields  $\phi$  and  $\Phi$  are massive, which reflects

the screening of static electric and scalar fields in the plasma. Hence, the Lagrangian of ESQED is

$$\begin{aligned} L_{\text{ESQED}} = & \frac{1}{4} F_{ij} F_{ij} + (\mathcal{D}_i \phi)^y (\mathcal{D}_i \phi) + M^2 (\phi)^y \phi + \frac{E(\phi)}{6} (\phi^y)^2 + \frac{1}{2} (\mathcal{G}_i \phi)^2 \\ & + \frac{1}{2} m_E^2 (\phi)^2 + \frac{A(\phi)}{24} \phi^4 + h_E^2 (\phi)^y \phi^2 + L_{\text{gf}} + L_{\text{gh}} + L : \end{aligned} \quad (17)$$

The term  $L_{\text{ESQED}}$  represents all other terms in ESQED which can be constructed out of the fields and respect the symmetries. Examples of such terms are  $h(\phi)^2 F_{ij}^2$  and  $g(\phi)(\phi^y)^3$ .

The second three-dimensional effective field theory is named magnetostatic scalar electrodynamics (MSQED) and consists of the fields  $\tilde{\phi}$  and  $A_i^{3d}$ . The symmetry is a gauged  $U(N)$  symmetry, exactly as in full SQED. The Lagrangian of MSQED then reads

$$L_{\text{MSQED}} = \frac{1}{4} F_{ij} F_{ij} + (\mathcal{D}_i \tilde{\phi})^y (\mathcal{D}_i \tilde{\phi}) + M^2 (\tilde{\phi})^y \tilde{\phi} + \frac{M(\tilde{\phi})}{6} (\tilde{\phi}^y)^2 + L_{\text{gf}} + L_{\text{gh}} + L_{\text{MSQED}} : \quad (18)$$

The term  $L_{\text{MSQED}}$  includes all operators that can be made out of  $A_i$  and  $\tilde{\phi}$ , for instance  $c(\phi)(F_{ij} F_{ij})^2$ . In the equations above, we have indicated that the parameters generally depend on  $\phi$ , which is the ultraviolet cut-off of the effective theory. This cut-off dependence is necessary in order to cancel the  $\phi$ -dependence which arises in perturbative calculations using the effective theory.

Let us close this section by motivating the study of this field theory given by (8). In the introduction we mentioned that the order of the phase transition may depend on the number of scalars  $N$  in the theory. These expectations arise from the study of the  $\epsilon$ -expansion [24]. The  $\epsilon$ -expansion generalizes the three spatial dimensions to 4 dimensions. One then solves the theory when  $\epsilon$  is small and then extrapolates to four dimensions, i.e. to  $\epsilon = 1$ . The  $\epsilon$ -expansion is not necessarily well behaved at  $\epsilon = 1$ . For pure  $g^2 = 4$  it is very successful and has predicted critical exponents in good agreement with other methods [24].

The infrared behaviour can be studied by looking at the renormalization group flow of the couplings of the relevant operators. The one-loop renormalization group equations in 4 dimensions read [24]:

$$\frac{d\epsilon^2}{d\ln\mu} = -\epsilon^2 \frac{N\epsilon^4}{24\epsilon^2}; \quad (19)$$

$$\frac{d\epsilon^2}{d\ln\mu} = \frac{(N+4) - 18\epsilon^2 + 54\epsilon^4}{24\epsilon^2}; \quad (20)$$

The point is that the renormalization group equations have a nontrivial infrared fixed point in 4 dimensions for  $N > N_c$ , where  $N_c \approx 365.9$ . Such fixed points are taken



as evidence for a second order phase transition, since the theory looks the same on all distance scales [27]. According to Ref. [24] the  $\epsilon$ -expansion is not so well behaved when the number of fields  $N$  become large. So it is of great interest to study this system by other means. The results presented in this work are a first step in this direction.

### 3 Short-distance Coefficients

In this section we determine the short-distance coefficients  $m_E^2(\epsilon)$  and  $M^2(\epsilon)$  to next-to-leading order in the parameters  $\epsilon^2$ ,  $\epsilon$  and  $e^2$ . We also compute the parameters  $\epsilon_E(\epsilon)$ ,  $e_E^2(\epsilon)$  and  $h_E^2(\epsilon)$  to next-to-leading order, as well as the coefficient  $\gamma_A(\epsilon)$  to leading order.

In the present work we shall use naive or strict perturbation [17] to determine the parameters in the effective theory. The Lagrangian of SQED is split according to

$$\begin{aligned} (\mathcal{L}_{\text{SQED}})_0 &= \frac{1}{4} F_{ij} F_{ij} + (\partial_\mu \phi)^\dagger (\partial^\mu \phi) + \mathcal{L}_{\text{gf}} + \mathcal{L}_{\text{gh}}; \\ (\mathcal{L}_{\text{SQED}})_{\text{int}} &= -\frac{1}{2} \phi^\dagger \phi + e^2 \phi^\dagger \phi A^2 - ieA_\mu (\phi^\dagger \partial^\mu \phi - \partial^\mu \phi^\dagger \phi) + \frac{1}{6} (\phi^\dagger \phi)^2; \end{aligned} \quad (21)$$

Although the strict perturbation expansion breaks down at distance scales  $R \sim 1/T$ , we can use it as device determining the short-distance coefficients in the effective Lagrangian. The idea is that physical quantities receive contributions from three momentum scales  $T$ ,  $eT$  and  $e^2 T$ . The parameters of ESQED are insensitive to the scales  $eT$  and  $e^2 T$  but encode the physics at the scale  $T$ . However, in the matching calculations we must make the same incorrect assumptions about the long-distance behaviour in the effective theory. If we tune the parameters so that the two theories are equal at long distances, then the infrared divergences in full SQED are identical to those encountered in ESQED. Of course, in perturbative calculations, one must regularize the infrared divergences by an infrared cutoff. In the present work dimensional regularization is used. In the effective theory these incorrect assumptions amounts to treating the mass parameters as well as other operators as perturbations. Strict perturbation theory is then defined by the following decomposition of the Lagrangian of ESQED

$$\begin{aligned} (\mathcal{L}_{\text{ESQED}})_0 &= \frac{1}{4} F_{ij} F_{ij} + (\partial_i \phi)^\dagger (\partial_i \phi) + \frac{1}{2} (\partial_i \phi)^\dagger (\partial_i \phi) + \mathcal{L}_{\text{gf}} + \mathcal{L}_{\text{gh}}; \\ (\mathcal{L}_{\text{ESQED}})_{\text{int}} &= M^2(\epsilon) \phi^\dagger \phi + \frac{1}{2} m_E^2(\epsilon) (\phi^\dagger \phi)^2 + \frac{\epsilon_E(\epsilon)}{6} (\phi^\dagger \phi)^3 + e_E^2(\epsilon) \phi^\dagger \phi A^2 + \\ &\quad h_E^2(\epsilon) \phi^\dagger \phi^2 + ie_E(\epsilon) A_\mu (\phi^\dagger \partial^\mu \phi - \partial^\mu \phi^\dagger \phi) + \frac{\gamma_A(\epsilon)}{24} (\phi^\dagger \phi)^4 + \mathcal{L}: \end{aligned} \quad (22)$$

In full SQED, wiggly and solid lines denote the propagators of photons and charged scalars, respectively. In ESQED, the same conventions apply. Moreover, dashed lines denote the

propagators of the real scalar field  $\phi$ . A cross in the Feynman diagrams denotes the insertion of the operator  $\phi^2$ . Note also that the figures only display those diagrams in the perturbative expansion which are non-vanishing in the Landau gauge.

### 3.1 Field Normalization Constants

When we match static correlators in the two theories, it is necessary to take into account the different normalization of the fields in 3d and 4d. The relation (16) breaks down beyond leading order in the couplings. The correction is due to the wave function renormalization of the fields in the full theory and can be read off from the momentum dependent part of the propagator. In the present work we shall need the relation of the fields at next-to-leading order in  $\alpha$  and  $e^2$ .

We denote the static self-energy function of the scalar field by  $\Pi(k)$ , and the static polarization tensor of the gauge field by  $\Pi_{ij}(k)$ . Now,  $\Pi(k)$  and  $\Pi_{ij}(k)$  can be expanded in number of loops in the loop expansion and can also be expanded in powers of the external momentum  $k$ . If we denote the  $n$ 'th order contribution to the scalar self-energy function by  $\Pi^{(n)}(k)$ , we can write

$$\Pi(k) = \Pi^{(1)}(0) + k^2 \Pi^{(1)0}(0) + \Pi^{(2)}(0) + O(k^4=T^2); \quad (23)$$

The corresponding relations for the various component of the photon polarization tensor read

$$\Pi_{00}(k) = \Pi_{00}^{(1)}(0) + k^2 \Pi_{00}^{(1)0}(0) + \Pi_{00}^{(2)}(0) + O(k^4=T^2); \quad (24)$$

$$\Pi_{ij}(k) = (k^2 \delta_{ij} - k_i k_j) \Pi^{10}(0) + \Pi^{20}(0) + O(k^4=T^2); \quad (25)$$

The fact that the infrared limit of  $\Pi_{ij}(k)$  ( $\Pi_{ij}^{(n)}(0) = 0$  for all  $n$ ) is zero reflects that spatial magnetic fields are not screened in the plasma. The relations between the fields in the two theories to next-to-leading order are [21]

$$\phi = \sqrt{\frac{h}{P}} \frac{1}{T} \left( 1 + \Pi^{(1)0}(0) \frac{i_{1=2}}{T} \right); \quad (26)$$

$$A_0 = \sqrt{\frac{A_0 h}{P}} \frac{1}{T} \left( 1 + \Pi_{00}^{(1)0}(0) \frac{i_{1=2}}{T} \right); \quad (27)$$

$$A_i^{3d} = \sqrt{\frac{A_i h}{P}} \frac{1}{T} \left( 1 + \Pi^{(1)0}(0) \frac{i_{1=2}}{T} \right); \quad (28)$$

The one-loop diagrams contributing to the self-energy of the scalar field is shown in Fig. 2, and read

$$\Pi^{(1)}(k) = \frac{2(N+1)}{3} \frac{P^Z}{P} \frac{1}{P^4} + \frac{(N+1)}{3} \frac{P^Z}{P} \frac{1}{P^2} + (d-1) e^2 \frac{P^Z}{P} \frac{1}{P^2}$$

$$e^{\frac{Z}{P}} \frac{4k^2}{P^2 (P+K)^2} - e^{\frac{Z}{P}} \frac{4(pk)^2}{P^4 (P+K)^2} : \quad (29)$$

Expanding in powers of the external momentum  $k$  gives

$$^{(1)}(k) = \frac{2(N+1)}{3} e^{\frac{Z}{P}} \frac{1}{P^4} + \frac{(N+1)}{3} e^{\frac{Z}{P}} \frac{1}{P^2} + e^2 (d-1) e^{\frac{Z}{P}} \frac{1}{P^2} \quad (30)$$

$$3e^2 k^2 e^{\frac{Z}{P}} \frac{1}{P^4} + O(k^4=T^2) : \quad (31)$$

From (30) we immediately get

$$^{(1)}(k) = \frac{2(N+1)}{3} e^{\frac{Z}{P}} \frac{1}{P^4} + \frac{(N+1)}{3} e^{\frac{Z}{P}} \frac{1}{P^2} + e^2 (d-1) e^{\frac{Z}{P}} \frac{1}{P^2} \quad (32)$$

$$^{(1)0}(k) = 3e^2 e^{\frac{Z}{P}} \frac{1}{P^4} + O(k^4=T^2) : \quad (33)$$

The sum-integral in (33) is ultraviolet divergent and the divergence is removed by the field strength renormalization counterterm, To leading order we have

$$Z = 1 + \frac{3e^2}{16\pi^2} ; \quad (34)$$

We then obtain the relation between the charged scalar fields in SQED and ESQED

$$\phi = \frac{1}{\sqrt{Z}} \phi_{\text{ESQED}} \quad (35)$$

Let us next move to the gauge field. The one-loop diagrams which contribute to the photon polarization tensor are displayed in Fig. 3, and one finds

$$(0;k) = 2N e^2 e^{\frac{Z}{P}} \int \frac{d^4k}{(2\pi)^4} \frac{(2p+k)(2p+k)}{P^2 (K+P)^2} : \quad (36)$$

Expanding to order  $k^2$  and integrating by parts, we get

$$^{(1)}_{00}(k) = 2N e^2 e^{\frac{Z}{P}} \frac{1}{P^2} - 4N e^2 e^{\frac{Z}{P}} \frac{p_0^2}{P^4} + \frac{4N e^2 k^2 e^{\frac{Z}{P}}}{3} \frac{p_0^2}{P^6} + O(k^4=T^2) ; \quad (37)$$

$$^{(1)}_{ij}(k) = \frac{N e^2 k^2}{3} (\delta_{ij} - \frac{k_i k_j}{k^2}) e^{\frac{Z}{P}} \frac{1}{P^4} + O(k^4=T^2) : \quad (38)$$

We can then read off  $^{(1)}_{00}(0)$ ,  $^{(1)0}_0(0)$  and  $^{(1)0}(0)$

$$^{(1)}_{00}(0) = 2N e^2 e^{\frac{Z}{P}} \frac{1}{P^2} - 4N e^2 e^{\frac{Z}{P}} \frac{p_0^2}{P^4} ; \quad (39)$$

$$^{(1)0}_{00}(0) = \frac{4N e^2 e^{\frac{Z}{P}}}{3} \frac{p_0^2}{P^6} ; \quad (40)$$

$$^{(1)0}(0) = \frac{N e^2 e^{\frac{Z}{P}}}{3} \frac{1}{P^4} : \quad (41)$$

Similarly, we carry out wave function renormalization of the gauge field by employing

$$Z_A = 1 - \frac{N e^2}{48 \pi^2}; \quad (42)$$

The relations between the fields in 3d and 4d then become

$$\phi(\vec{p}) = \sqrt{\frac{1}{T}} A_0^h(\vec{p}) + \frac{N e^2}{3(4\pi)^2} \left( \ln \frac{1}{4T} + \frac{1}{E} + 1 \right) \phi^i(\vec{p}); \quad (43)$$

$$A_i^{3d}(\vec{p}) = \sqrt{\frac{1}{T}} A_i^h(\vec{p}) + \frac{N e^2}{3(4\pi)^2} \left( \ln \frac{1}{4T} + \frac{1}{E} \right) \phi^i(\vec{p}); \quad (44)$$

### 3.2 Mass parameters

In this subsection we calculate the mass parameters in the effective Lagrangian at next-to-leading order in the coupling constants. There are several ways of determining the mass parameters. One way is to match the propagator of the zero-frequency mode in the full theory with the propagator in ESQED. We need the mass parameter at next-to-leading order in the parameters  $\pi^2$ ,  $\pi$  and  $e^2$ . Let us denote the static two-point function of the Higgs field in SQED by  $\Pi_{11}^{SQED}(k)$ . Since we can expand the self-energy function in both powers of the external momentum and number of loops we can write

$$\Pi_{11}^{SQED}(k) = k^2 + \pi^2 + \Pi^{(1)}(k) + k^2 \Pi^{(1)0}(k) + \Pi^{(2)}(k); \quad (45)$$

Similarly, we denote the two-point function of the Higgs field in ESQED by  $\Pi_{11}^{ESQED}(k)$ . We can then write

$$\Pi_{11}^{ESQED}(k; \pi) = k^2 + M^2(\pi) + \pi^2; \quad (46)$$

Here, we have added a mass counterterm  $M^2$ , which is associated with mass renormalization. The matching requirement is then

$$\Pi_{11}^{SQED}(k) = 1 + \frac{1}{k^2} \Pi^{(1)0}(0) \frac{1}{k^2} \Pi_{11}^{ESQED}(k) \quad (47)$$

The factor  $1 + \frac{1}{k^2} \Pi^{(1)0}(0) \frac{1}{k^2}$  takes care of the different normalization of the fields. Solving for the mass parameter, we obtain

$$M^2(\pi) = \pi^2 \frac{1}{1 + \frac{1}{k^2} \Pi^{(1)0}(0) \frac{1}{k^2}} + \frac{1}{k^2} \Pi^{(1)0}(0) \frac{1}{k^2} \Pi_{11}^{ESQED}(k) + \Pi^{(2)}(0) \quad (48)$$

$\Pi^{(1)}(0)$  and  $\Pi^{(1)0}(0)$  are given by (32) and (33). The two-loop contributions to the scalar self-energy are depicted in Fig. 4 and yield

$$\begin{aligned} \Pi^{(2)}(0) = & \frac{(N+1)^2 \pi^2}{9} \frac{1}{P_Q} \frac{1}{P^2 Q^4} - 2(d-2)N e^2 \frac{1}{P_Q} \frac{1}{P^2 Q^4} \\ & (d-1) \frac{(N+1) e^2 \pi^2}{3} \frac{1}{P_Q} \frac{1}{P^2 Q^4}; \end{aligned} \quad (49)$$

The parameter  $\mu^2$ , and the coupling constants  $\alpha$  and  $e^2$  are renormalized by the substitutions

$$Z_2 = 1 + \frac{(N+1)}{3(4-\epsilon)^2} \frac{3e^2}{(4-\epsilon)^2}; \quad (50)$$

$$Z_3 = 1 + \frac{(N+4)}{3(4-\epsilon)^2} \frac{18\epsilon^2 + 54e^4}{(4-\epsilon)^2}; \quad (51)$$

$$Z_{e^2} = 1 + \frac{N e^2}{3(4-\epsilon)^2}; \quad (52)$$

We are still left with a pole in  $\epsilon$ . This divergence is cancelled by the mass counterterm, which thereby is determined to be

$$M^2 = \frac{(N+1)\mu^2 T^2}{36(4-\epsilon)^2} \frac{6(N+1)\epsilon^2 T^2 + 9(N+5)e^4 T^2}{(4-\epsilon)^2}; \quad (53)$$

This gives the mass parameter  $M^2(\mu)$  to two-loop order:

$$\begin{aligned} M^2(\mu) = & \mu^2 \left( 1 + \frac{1}{(4-\epsilon)^2} \frac{h}{6e^2} \frac{2(N+1)}{3} \ln \frac{\mu}{4T} + \frac{(N+1)}{36} \frac{T^2}{\mu^2} + \right. \\ & \frac{e^2 T^2}{4} + \frac{(N+1)T^2}{108} \frac{h}{16\epsilon^2} \frac{2(N+4)}{4} \ln \frac{\mu}{4T} + 12 \ln \frac{\mu}{4T} \\ & 2(N+1) \frac{h}{\epsilon} + 6 + 6 \frac{0(1)}{(1)} \frac{i}{(1)} \\ & \frac{(N+1)T^2}{12} \frac{e^2 h}{16\epsilon^2} \frac{4 \ln \frac{\mu}{4T} + 8 \ln \frac{\mu}{4T} + \frac{10}{3} + 4 \frac{0(1)}{(1)} \frac{i}{(1)}}{16\epsilon^2} \\ & \frac{T^2}{36} \frac{e^4 h}{16\epsilon^2} \frac{(42N+36) \ln \frac{\mu}{4T} + 36(N+5) \ln \frac{\mu}{4T} + (54-24N) \frac{h}{\epsilon} +}{72+28N+(90+18N) \frac{0(1)}{(1)} \frac{i}{(1)}} : \end{aligned}$$

Note that we have used the renormalization group equations,

$$\frac{d}{d\mu} = \frac{(N+4)\epsilon^2}{24\epsilon^2} \frac{18\epsilon^2 + 54e^4}{(4-\epsilon)^2}; \quad \frac{de^2}{d\mu} = \frac{N e^4}{24\epsilon^2}; \quad (54)$$

to change the scale from  $\mu$  to  $\mu'$ . There is a remaining dependence on  $\mu$ , which shows that  $M^2(\mu)$  depends explicitly upon the factorization scale. This is necessary in order to cancel the  $\epsilon$ -dependence which arises in the effective theory.

Let us now turn to the mass parameter  $m_E^2(\mu)$ . This parameter has previously been determined for  $N=1$  by the present author to next-to-leading order in Ref. [29] using

the Feynman gauge. For completeness we include the calculations here. It is also a good check that we obtain the same result in the Landau gauge.

This parameter is determined by matching the propagator of the zero-frequency mode of the timelike component of the gauge with the propagator of the real scalar field in ESQED. In complete analogy with the calculations of the scalar mass parameter, we find

$$m_E^2(\mu) = \Pi_{00}^{(1)}(0) + \Pi_{00}^{(1)}(0) - \Pi_{00}^{(1)0}(0) - \Pi_{00}^{(1)}(0): \quad (55)$$

Now, the expressions for  $\Pi_{00}^{(1)}(0)$  and  $\Pi_{00}^{(1)0}(0)$  are given by (39) and (40), while the two-loop part of the self-energy of  $A_0$  is given by the displayed graphs in Fig. 5. Many of the two-loop sum-integrals vanish in dimensional regularization, while others factorize into products of one-loop sum-integrals. After some calculations we find

$$\begin{aligned} \Pi_2(0) = & 8(d-1)N e^{\frac{Z}{P}} \frac{p_0^2}{P^6 Q^2} - 2(d-1)N e^{\frac{Z}{P}} \frac{1}{P^4 Q^2} \\ & - \frac{2N(N+1)e^{\frac{Z}{P}}}{3} \frac{1}{P^4 Q^2} + \frac{8N(N+1)e^{\frac{Z}{P}}}{3} \frac{p_0^2}{P^6 Q^2}: \end{aligned} \quad (56)$$

The above sum-integrals are individually ultraviolet divergent. However, the poles in cancel, and we are left with a finite result for  $\Pi_{00}^{(2)}(0)$ :

$$\Pi_2(0) = \frac{N e^4 T^2}{(4\pi)^2} + \frac{N(N+1)e^2 T^2}{144\pi^2}: \quad (57)$$

The reason behind the fact that we get a finite result before renormalization is that the two counterterm diagrams cancel against each other as a consequence of the Ward identity. Using these results, we finally obtain  $m_E^2(\mu)$  to order  $e^4$  and order  $e^2$ :

$$m_E^2(\mu) = \frac{N e^2 T^2}{3} \ln \frac{\mu}{T} + \frac{2N e^2}{3(4\pi)^2} \ln \frac{\mu}{4T} + \frac{3e^2}{(4\pi)^2} + \frac{N(N+1)e^2 T^2}{144\pi^2}: \quad (58)$$

In contrast with the scalar mass parameter,  $m_E^2(\mu)$  has no explicit dependence on  $\beta$ . This is easily verified by using the renormalization group equation for the gauge coupling  $e$ .

### 3.3 Coupling Constants

In this subsection we shall determine the coupling constants  $e_E(\mu)$ ,  $e_E^2(\mu)$  and  $h_E^2(\mu)$  to next-to-leading order in the coupling constants of the full theory. We also compute the coupling constant  $g_A(\mu)$  to leading order.

Let us first consider the coefficient  $e_E(\mu)$ . To leading order one can simply read off this parameter from the full theory. Substituting  $\beta = \frac{1}{T}$  into (8) and comparing with

the Lagrangian of ESQED we find

$$\Gamma_E(k) = T : \quad (59)$$

One way to calculate the coupling  $\Gamma_E(k)$  beyond leading order, is by matching the static four-point of the Higgs field in full SQED with the four-point function of the Higgs field in ESQED. This is complicated by the breakdown of the simple relation (35). At next-to-leading order it is sufficient to take into account the short-distance coefficient which multiplies .

We denote the four-point of the Higgs field in SQED by  $\Gamma_{1;1;1;1}^{SQED}(k)$ , where  $k$  collectively denotes the external momenta. The one-loop correction to the four-point function is given by the Feynman diagrams in Fig. 6. Taken at zero external momenta, one finds

$$\Gamma_{1;1;1;1}^{SQED}(0) = \frac{(N+4)}{3} T^2 \frac{1}{K^4} + 6(d-1) e^2 T^2 \frac{1}{K^4} : \quad (60)$$

In ESQED, we denote the corresponding four-point function by  $\Gamma_{1;1;1;1}^{ESQED}(k)$ . Since all the fields are massless in the strict perturbation expansion and all diagrams are taken at vanishing external momenta, there is no scale in the integrals. Thus the loop corrections to  $\Gamma_{1;1;1;1}^{ESQED}(0)$  vanish:

$$\Gamma_{1;1;1;1}^{ESQED}(0) = \Gamma_E(k) : \quad (61)$$

Taking into account the short-distance coefficient multiplying the field, the matching leads to the following equation

$$\Gamma_E(k) = T^2 \frac{(N+4)}{3} T^2 \frac{1}{P^4} + 6 e^2 T^2 \frac{1}{P^4} + 6(d-1) e^4 T^2 \frac{1}{P^4} : \quad (62)$$

Renormalization of the quartic coupling is again carried out by the substitution  $1 \rightarrow Z$  in the first term on the right hand side of (62). This yields

$$\Gamma_E(k) = T^2 \frac{(N+4)^2}{24} \frac{1}{Z^2} + \frac{18 e^2 + 54 e^4}{24} \left( \ln \frac{1}{4T} + \Gamma_E(k) \right) + \frac{3 e^4}{4} \frac{1}{Z^2} : \quad (63)$$

The couplings  $e_E^2(k)$  and  $h_E^2(k)$  are computed by matching the correlators  $\Gamma_{1;1;1;1}^{SQED}(k)$  and  $\Gamma_{1;1;1;1}^{SQED}(k)$  in full SQED with the corresponding correlators in ESQED. The relevant diagrams are displayed in Fig. 7. Calculated at zero external momenta one finds the following results in SQED in the one-loop approximation:

$$\Gamma_{1;1;1;1}^{SQED}(0) = e^2 + 8 e^4 \frac{1}{P^4} + \frac{e^2 (N+3)}{3} \frac{1}{P^4} + \frac{e^4 (N+3)}{3} \frac{1}{P^4} : \quad (64)$$

$$\Gamma_{1;1;1;1}^{SQED}(0) = e^2 + 8 e^4 \frac{1}{P^4} + \frac{e^2 (N+3)}{3} \frac{1}{P^4} + \frac{e^4 (N+3)}{3} \frac{1}{P^4} : \quad (65)$$

In MSQED we know that the one-loop correction to the correlators vanish, since all internal fields are massless and the external momenta are zero. Taking into account the different normalization of the fields in SQED and ESQED, we find

$$e_E^2(\mu) = e^2 T \left[ \frac{N}{3} e^4 T_P^Z \frac{1}{P^4} + \frac{e^2 (N+3)}{3} T_P^Z \frac{h_{ij} p_i p_j}{4 P^6} - \frac{1}{P^4} \right]; \quad (66)$$

$$h_E^2(\mu) = e^2 T \left[ \frac{N}{3} e^4 T_P^Z \frac{1}{P^4} + \frac{e^2 (N+3)}{3} T_P^Z \frac{h_{ij} p_i p_j}{4 P^6} - \frac{1}{P^4} \right]; \quad (67)$$

We notice that the term involving  $\ln(0)$  cancels against the second term in (64), after we have integrated by parts. This reflects the Ward identity. In the corresponding expression for  $h_E^2(\mu)$ , there is not a complete cancellation, but we are left with a finite contribution. To render the result finite we carry out charge renormalization in the usual way. Using Appendix A, the final results are

$$e_E^2(\mu) = e^2 T \left[ \frac{N e^2}{24 \mu^2} \left( \ln \frac{\mu}{4 T} + \frac{1}{\epsilon_E} \right) \right]; \quad (68)$$

$$h_E^2(\mu) = e^2 T \left[ \frac{N e^2}{24 \mu^2} \left( \ln \frac{\mu}{4 T} + \frac{1}{\epsilon_E} + 1 \right) + \frac{(N+3)}{48 \mu^2} + \frac{e^2}{8 \mu^2} \right]; \quad (69)$$

We close this section by computing the coefficient in front of the operator  $\mathcal{O}_A$ . To leading order in the couplings of full SQED,  $\mathcal{A}_A(\mu)$  is given by the one-loop contribution to the four-point function for timelike photons at zero external momenta. This correlator is denoted by  $\mathcal{A}_{A_0 A_0 A_0 A_0}^{\text{SQED}}(k)$ . The matching condition then reads

$$\mathcal{A}_A(\mu) = T \mathcal{A}_{A_0 A_0 A_0 A_0}^{\text{SQED}}(0); \quad (70)$$

The one-loop graphs contributing to this correlator are displayed in Fig. 8. One obtains

$$\mathcal{A}_{A_0 A_0 A_0 A_0}^{\text{SQED}}(k) = 12N e^4 T_P^Z \frac{1}{P^4} + 96N e^4 T_P^Z \frac{p_0^2}{P^6} - 96N e^4 T_P^Z \frac{p_0^4}{P^8}; \quad (71)$$

Again the sum-integrals are divergent term by term, but the poles in  $\epsilon$  cancel in the final result. This is also the case in QED and QCD [14]. Using Appendix A, we find

$$\mathcal{A}_A(\mu) = \frac{N e^4 T}{2}; \quad (72)$$

Finally, we note that the four coupling constants  $e_E^2(\mu)$ ,  $e_E^2(\mu)$ ,  $h_E^2(\mu)$  and  $\mathcal{A}_A(\mu)$  are renormalization group invariant at next-to-leading order in the coupling constants of SQED. Thus, we can trade the scale  $\mu$  for arbitrary renormalization scale  $\mu_R$ .



## 4 Middle-distance Coefficients

In this section we determine the middle-distance coefficients of MSQED, which is given by (18). We know from general renormalization theory that MSQED can reproduce the correlators in ofESQED at long distances  $R \gg 1/eT$  to any desired accuracy by adding sufficiently many operators and tuning their coefficients as functions of the parameters ofESQED. The middle-distance coefficients are sensitive to momentum scales  $T$  and  $eT$ . The scale  $T$  has already been encoded in the parameters by the matching which was carried out in the previous section. In order to treat the physics on the scale  $eT$  correctly, we must include the mass parameter  $m_E^2(\mu)$  in the free part of the Lagrangian. By doing this, we treat the effects of  $m_E^2(\mu)$  to all orders, while the other parameters in ESQED are treated as perturbations. In particular this means that the scalar mass parameter is treated as a perturbation. Of course, this way of doing perturbative calculations is also afflicted with infrared divergences. However, these divergences are screened at the scale  $e^2T$ , to which the parameters of MSQED are insensitive. As long as we make the same incorrect assumptions about the long-distance behaviour in MSQED, we can use this method to determine the middle-distance coefficients of MSQED.

According to the discussion above, the Lagrangian ofESQED is split into a free and an interacting piece:

$$(\mathcal{L}_{\text{ESQED}})_0 = \frac{1}{4}F_{ij}F_{ij} + (\partial_i^y)(\partial_i^y) + \frac{1}{2}(\partial_i^y)^2 + \frac{1}{2}m_E^2(\mu)^2 + L_{gf} + L_{gh}; \quad (73)$$

$$\begin{aligned} (\mathcal{L}_{\text{ESQED}})_{\text{int}} = & M^2(\mu)^y + \frac{e(\mu)}{6}(\partial^y)^2 + e_E^2(\mu)^y A_i^2 + h_E^2(\mu)^y \partial^2 \\ & + ie_E(\mu)A_i(\partial^y\partial_i - \partial^i\partial_y) + \frac{A(\mu)}{24}\partial^4 + L: \end{aligned} \quad (74)$$

Using strict perturbation theory the Lagrangian ofMSQED is split in a way that is now familiar:

$$\begin{aligned} (\mathcal{L}_{\text{MSQED}})_0 = & \frac{1}{4}\tilde{F}_{ij}\tilde{F}_{ij} + (\partial_i^y\tilde{~})^y(\partial_i^y\tilde{~}) + L_{gf} + L_{gh}; \\ (\mathcal{L}_{\text{MSQED}})_{\text{int}} = & M^2(\mu)^{\sim y\sim} + e_M^2(\mu)^{\sim y\sim} \tilde{A}_i^{3d}\tilde{A}_i^{3d} + ie_M(\mu)\tilde{A}_i(\tilde{~}^y\partial_i\tilde{~} - \tilde{~}^i\partial_y\tilde{~}) + \\ & \frac{M(\mu)}{6}(\tilde{~}^y\tilde{~})^2 + L^0: \end{aligned} \quad (75)$$

In MSQED, wiggly and solid lines denote the propagators of photons and charged scalars, respectively. Again, we only show the diagrams which are nonzero in the Landau gauge.

## 4.1 Field Normalization Constants

In the tree approximation the fields in ESQED and MSQED are related as

$$\tilde{\phi}(\mathbf{k}) = \phi(\mathbf{k}); \quad \tilde{A}_i(\mathbf{k}) = A_i(\mathbf{k}); \quad (76)$$

Again the field normalization constant can be read off from the momentum dependent part of the underlying theory, which in this case is ESQED. Consider first the scalar field. In strict perturbation theory it is consistent to make a series expansion of the propagator in powers of the external momentum  $k$ . The only mass scale provided in the loop integrals of ESQED is then the mass  $m_E^2(\mu)$ . Since the only one-loop diagram involving the field  $\phi$  is independent of the external momentum (the tadpole in Fig. 9), the one-loop correction to the momentum dependent part of the propagator vanishes. Hence there is no renormalization of the field  $\tilde{\phi}$ .

A similar argument holds for the gauge field: Since the interaction between the fields  $A_i$  and  $\phi$  gives rise to momentum dependent graphs first at the two-loop level, there is no renormalization of  $\tilde{A}_i$  at leading order in the coupling constants, Thus, (76) holds to next-to-leading order.

## 4.2 Mass Parameter

In this subsection we determine the scalar mass parameter in the two-loop approximation. We calculate  $\tilde{M}^2(\mu)$  by matching the Higgs propagator in ESQED,  $\tilde{\Delta}_{1;1}^{\text{ESQED}}(k)$  with the Higgs propagator in MSQED,  $\Delta_{1;1}^{\text{MSQED}}(k)$ . The diagrams contributing to the two-point function in the strict perturbation expansion of ESQED are displayed in Fig. 9. After Taylor expanding the self-energy function in ESQED in powers of  $k^2$ , the mass  $m_E^2(\mu)$  is the only mass scale in the loop diagrams. This implies that all loop diagrams which does not involve the field  $\phi$  vanish in dimensional regularization. The two-point function in ESQED then reads

$$\begin{aligned} \tilde{\Delta}_{1;1}^{\text{ESQED}}(k) &= k^2 + \tilde{M}^2(\mu) + e_E^2 \int \frac{1}{p^2 + m_E^2} \\ &\quad - 2e_E^4 \int \frac{1}{(p^2 + m_E^2)(q^2 + m_E^2)(p-q)^2} : \end{aligned} \quad (77)$$

The one-loop diagrams in MSQED are the same as in ESQED, except for those diagrams which involve the real scalar field  $\phi$ . Thus, the loop corrections to scalar self-energy function in strict perturbation theory, vanish and the only non-vanishing contribution comes from the mass counterterm  $\tilde{M}^2$ , which cancels the logarithmic ultraviolet divergences

$$\Delta_{1;1}^{\text{MSQED}}(k) = k^2 + \tilde{M}^2(\mu) + \tilde{M}^2 : \quad (78)$$

Matching the two expressions, (77) and (78) we find

$$\tilde{M}^2(\mu) = M^2(\mu) + e_E^2 \int \frac{1}{p^2 + m_E^2} - 2e_E^4 \int \frac{1}{(p^2 + m_E^2)(q^2 + m_E^2)(p - q)^2} \quad (79)$$

The integrals are tabulated in Appendix B. The two-loop integral is ultraviolet divergent. The pole in  $\mu$  must then be canceled by the mass counterterm, which then is determined to be

$$\tilde{M}^2 = \frac{e_E^4}{2(4\pi)^2} : \quad (80)$$

Our final expression for the scalar mass parameter in MSQED is

$$\tilde{M}^2(\mu) = M^2(\mu) - \frac{e_E^2 T m_E}{4} - \frac{e_E^4}{16\pi^2} \left( 1 + 2 \ln \frac{\mu}{2m_E} \right) : \quad (81)$$

### 4.3 Coupling Constants

In this subsection we determine the gauge coupling  $e_M^2(\mu)$  and the quartic coupling  $\lambda_M(\mu)$  to next-to-leading order in the parameters of ESQED. The matching is somewhat simplified, since the fields in MSQED can be directly identified with the fields in ESQED to next-to-leading order.

Consider first  $e_M^2(\mu)$ . This coefficient is determined by calculating the correlator  $\langle A_{iA_j} A_{iA_j} \rangle_{11}^{\text{ESQED}}(k)$  and matching with the corresponding correlator in MSQED,  $\langle A_{iA_j} A_{iA_j} \rangle_{11}^{\text{MSQED}}(k)$ . The one-loop corrections to this correlator in ESQED only involve massless fields. Since the correlators are calculated at vanishing external momenta, the regularized loop integrals vanish. This implies that the tree-level results holds also to next-to-leading order:

$$\langle A_{iA_j} A_{iA_j} \rangle_{11}^{\text{ESQED}}(0) = e_E^2(\mu) : \quad (82)$$

In MSQED, the same arguments apply equally well here, and we are left with

$$\langle A_{iA_j} A_{iA_j} \rangle_{11}^{\text{MSQED}}(0) = e_M^2(\mu) : \quad (83)$$

We then conclude

$$e_M^2(\mu) = e_E^2(\mu); \quad (84)$$

where  $e_E^2(\mu)$  is given by (68).

Let us next consider the coupling constant  $\lambda_M(\mu)$ . The quartic coupling  $\lambda_M(\mu)$  is determined by the following matching equation, in complete analogy with the calculations of  $e_E(\mu)$  in the subsection 3.3,

$$\langle A_{1111} A_{1111} \rangle_{1111}^{\text{ESQED}}(0) = \langle A_{1111} A_{1111} \rangle_{1111}^{\text{MSQED}}(0) : \quad (85)$$

The only one-loop diagram contributing to  $\Pi_{1111}^{\text{ESQED}}(k)$  at zero external momenta is displayed in Fig 10. Using Appendix B, we obtain the correlator in the one-loop approximation:

$$\begin{aligned}\Pi_{1111}^{\text{ESQED}}(0) &= \Pi_E(0) \frac{e_E^4}{4} \int \frac{1}{(p^2 + m_E^2)^2} \\ &= \Pi_E(0) \frac{e_E^4}{4 m_E^2} : \end{aligned} \quad (86)$$

In MSQED, the one-loop corrections to the correlator  $\Pi_{1111}^{\text{MSQED}}(k)$  at zero external momenta vanish, since there is no mass scale in the corresponding loop integrals. Using the matching equation 4.3 we finally end up with

$$\Pi_M(0) = \Pi_E(0) \frac{e_E^4}{4 m_E^2} : \quad (87)$$

Here,  $\Pi_E(0)$  is given by (63)

## 5 Summary

In the present paper we have discussed various approaches to dimensional reduction and the construction of effective three-dimensional field theories. The idea is basically to exploit the fact there is two or more well separated mass scales in the system and that the heavy degrees of freedom decouple at long distance leaving us with effective field theories of the light degrees of freedom. The effects of the heavy modes are to renormalize the parameters in the effective theory and induce new higher order interactions. The method of Braaten and Nieto is perhaps the most clean and transparent way of doing effective field theory. One advantage is that we do not distinguish explicitly between contributions from the static and nonstatic modes to a correlator.

In this work I have applied this method to a field theory consisting of  $N$  charged  $U(N)$  symmetric scalars coupled to an Abelian gauge field. I have presented the calculations of the parameters of ESQED and MSQED to next-to-leading order in the parameters  $g^2$ , and  $e^2$  of full SQED. The results appearing are a generalization of the existing results for the Abelian Higgs model, where  $N = 1$ .

The effective field theory (MSQED) that we have obtained can now be used to a nonperturbative study of the phase transition on the lattice. This includes in particular the order of the phase transition as a function of the number scalar fields  $N$ . The results could be compared to the findings of the  $\epsilon$ -expansion, and give some useful information of the applicability of this method.

## A Sum -integrals in the Full Theory

Throughout the work we use the imaginary time formalism, where the four-momentum is  $P = (p_0; \mathbf{p})$  with  $P^2 = p_0^2 + \mathbf{p}^2$ . The Euclidean energy takes on discrete values,  $p_0 = 2nT$  for bosons and  $p_0 = (2n+1)T$  for fermions. Dimensional regularization is used to regularize both infrared and ultraviolet divergences by working in  $d = 4 - 2\epsilon$  dimensions, and we apply the  $\overline{MS}$  renormalization scheme. We shall use the following notations for the sum -integrals that appear

$$\sum_P^Z f(P) = \frac{e^{-\epsilon - 2}}{4} T^X \sum_{p_0=2nT}^Z \frac{d^{3-2\epsilon} \mathbf{p}}{(2\epsilon)^{3-2\epsilon}} f(P); \quad (\text{A.1})$$

The one-loop sum -integrals needed in this work have been calculated in e.g. Ref. [11]. We list them here for the convenience of the reader:

$$\sum_P^Z \frac{1}{P^2} = \frac{T^2}{12} \frac{1}{4T} {}_2h_1 + 2 + 2 \frac{{}_0(1)}{(1)} + O(\epsilon^2)^1; \quad (\text{A.2})$$

$$\sum_P^Z \frac{1}{(P^2)^2} = \frac{1}{(4\epsilon)^2} \frac{1}{4T} {}_2h_1 - 2\epsilon + O(\epsilon^2)^1; \quad (\text{A.3})$$

$$\sum_P^Z \frac{p_0^2}{(P^2)^2} = \frac{T^2}{24} \frac{1}{4T} {}_2h_1 + 2 \frac{{}_0(1)}{(1)} + O(\epsilon^2)^1; \quad (\text{A.4})$$

$$\sum_P^Z \frac{p_0^2}{(P^2)^3} = \frac{1}{4(4\epsilon)^2} \frac{1}{4T} {}_2h_1 - 2 + 2\epsilon + O(\epsilon^2)^1; \quad (\text{A.5})$$

$$\sum_P^Z \frac{p_0^4}{(P^2)^4} = \frac{1}{8(4\epsilon)^2} \frac{1}{4T} {}_2h_1 + \frac{8}{3} + 2\epsilon + O(\epsilon^2)^1; \quad (\text{A.6})$$

A mold and Zhai [11], and Kastening and Zhai [12] have calculated and tabulated all the sum -integrals, except for the last one, in the list below.

$$\sum_{PP}^Z \frac{1}{P^2 Q^2 (P+Q)^2} = 0; \quad (\text{A.7})$$

$$\sum_{PP}^Z \frac{q_0^2}{P^4 Q^2 (P+Q)^2} = \frac{T^2}{12(4\epsilon)^2} + O(\epsilon^2); \quad (\text{A.8})$$

$$\sum_{PP}^Z \frac{p_0^2}{P^4 Q^2 (P+Q)^2} = 0; \quad (\text{A.9})$$

$$\sum_{PP}^Z \frac{p_0 q_0}{P^2 Q^4 (P+Q)^2} = 0; \quad (\text{A.10})$$

The last integral can, however, be found from the second and third by changing variables.

## B Integrals in the three Dimensional Theory

$$\int_P^Z f(P) = \frac{e^{\epsilon/2}}{4} \int^Z \frac{d^{3-2\epsilon} P}{(2)^{3-2\epsilon}} f(P): \quad (\text{B.1})$$

In the effective theory we need the following one-loop integrals

$$\int_P^Z \frac{1}{p^2 + m^2} = \frac{m}{4} \frac{1}{2m} \int^Z \frac{d^{3-2\epsilon} p}{(2)^{3-2\epsilon}} \frac{1}{p^2 + m^2} + O(\epsilon^2); \quad (\text{B.2})$$

$$\int_P^Z \frac{1}{(p^2 + m^2)^2} = \frac{1}{4m} \frac{1}{2m} \int^Z \frac{d^{3-2\epsilon} p}{(2)^{3-2\epsilon}} \frac{1}{p^2 + m^2} + O(\epsilon^2): \quad (\text{B.3})$$

All integrals are straightforward to evaluate in dimensional regularization. Details may be found in Ref. [30]. The specific two-loop integrals needed are

$$\int_{pq}^Z \frac{1}{(p^2 + m^2)(q^2 + m^2)(p - q)^2} = \frac{1}{16} \frac{1}{2} \frac{1}{4} + \frac{1}{2} + \frac{1}{2m} + O(\epsilon^2):$$

This integral have been computed by several authors, e.g. in Ref. [4].

## C Some Sample Calculations

All the sum-integrals needed in the present work have been calculated and tabulated in Ref. [11]. In order to illustrate the methods of Arnold Zhai, we explicitly calculate some one and two-loop sum-integrals.

Let us start with the following one-loop sum-integral:

$$\begin{aligned} \int_P^Z \frac{p_0^2}{(P^2)^m} &= \frac{e^{\epsilon/2}}{4} T_n^X \int^Z \frac{d^{3-2\epsilon} p}{(2)^{3-2\epsilon}} \frac{(2nT)^2}{[p^2 + (2nT)^2]^m} \\ &= \frac{e^{\epsilon/2}}{4} T(2T)^2 \int^Z \frac{d^{3-2\epsilon} p}{(2)^{3-2\epsilon}} \frac{1}{[p^2 + (2T)^2]^m} T_n^X n^{5-2m-2} \\ &= \frac{e^{\epsilon/2}}{4^{2T^2}} \frac{T^{6-2m}}{2^{2m-3}} \frac{\Gamma(3-2\epsilon)}{\Gamma(m)} (2m-5+2\epsilon): \quad (\text{C.1}) \end{aligned}$$

In the second line we have changed variables, and in the last line we have employed the definitions of the  $\Gamma$  and  $\Gamma$ -functions, as well as performing a standard one-integral using dimensional regularization [30]. By expanding in  $\epsilon$ , using  $m = 4$ , we obtain (A.6).

Let us next calculate a two-loop integral

$$\int_P^Z \frac{p_0^2}{P^4 Q^2 (P+Q)^2} = \int_P^Z \frac{p_0^2}{P^4} (P); \quad (C.2)$$

where we have defined the bosonic self-energy diagram

$$(P) = \int_Q^Z \frac{1}{Q^2 (P+Q)^2}; \quad (C.3)$$

The bosonic self-energy is ultraviolet divergent. This divergence arises at  $T = 0$ , so we must subtract off the temperature independent part:

$$(P) = {}^0(P) + {}^T(P); \quad (C.4)$$

The temperature independent part is, using standard results from dimensional regularization

$${}^0(P) = \int_Q^Z \frac{d^d q}{(2\pi)^d} \frac{1}{Q^2 (P+Q)^2} = \frac{1}{(4\pi)^2} \frac{4}{P^2} \left[ \frac{h_1}{\epsilon} + 2 + O(\epsilon) \right]; \quad (C.5)$$

By using (C.1) with  $m = 2 + \epsilon$ , we find

$$\int_P^Z \frac{p_0^2}{P^4} {}^0(P) = \frac{T^2}{24} \frac{1}{(4\pi)^2} \frac{h_1}{\epsilon} + 4 \frac{1}{4T} + 1 + 4 \frac{(-1)^i}{(\epsilon-1)}; \quad (C.6)$$

We now need  ${}^T(P)$  and in order to obtain it, we shall compute  $(P)$  and subtract off its  $T = 0$  limit. We shall evaluate the bosonic self-energy by using the propagator in coordinate space

$$(q_0; r) = \frac{e^{i q_0 r}}{4r}; \quad (C.7)$$

This form of the propagator is found by Fourier transforming the momentum space propagator in the usual way. The bosonic self-energy can now be written as

$$\begin{aligned} (P) &= T \sum_{q_0} \int_Q^Z d^3 r (q_0; r) (q_0 + p_0; r) e^{i p r} \\ &+ \frac{T}{(4\pi)^2} \sum_{q_0} \int_Q^Z \frac{d^3 r}{r^2} e^{i q_0 r} e^{i q_0 + p_0 r} e^{i p r}; \end{aligned} \quad (C.8)$$

The sum over Matsubara frequencies is given by

$$\sum_{q_0} e^{i q_0 + p_0 r} e^{i p r} = \frac{h}{\coth r + \frac{i}{p_0}} \quad (C.9)$$

Here,  $r = 2/rT$  and  $p_0 = p_0/(2/T)$ . This formula can be obtained by splitting the sum into three parts depending on the sign of  $q_0$  and  $(q_0 + p_0)$ , and then use known results for geometric series. Substituting (C.9) into (C.8) and letting  $T \rightarrow 0$ , we find the temperature independent part of the bosonic self-energy. Subtracting this from  $\Pi(P)$ , we find

$$\Pi^T(P) = \frac{T}{(4\pi)^2} \int_0^\infty \frac{d^3r^h}{r^2} \coth r - \frac{1}{r} e^{ip \cdot r} : \quad (C.10)$$

Although  $\Pi^T(P)$  is finite (by construction)  $p_0^2 \Pi^T = P^4$  is divergent in the ultraviolet because the former goes like  $1/P^2$  in this limit:

$$\Pi^T(P) \sim \frac{2}{P^2} \int_0^\infty \frac{1}{Q^2} : \quad (C.11)$$

This limit can be inferred by the contour trick [31]. One rewrites the sum over the Matsubara frequencies as a contour integral and studies its high temperature limit [11]. Moreover, the high momentum behaviour is also given by the small  $r$  behaviour of the integrand in (C.10). Using the series expansion of  $\coth r$ , we find

$$\Pi^T(P) \sim \frac{T}{3(4\pi)^2} \int_0^\infty \frac{d^3r}{r^2} r e^{ip \cdot r} : \quad (C.12)$$

We can now write the finite temperature part of the two loop diagram (C.2) as

$$\frac{T}{(4\pi)^2} \int_0^\infty \frac{1}{P^2} \int_0^\infty \frac{d^3r^h}{r^2} \coth r - 1 = r \int_{r=3r}^i e^{ip \cdot r} e^{ip_0 \cdot r} + 2 \int_0^\infty \frac{p_0^2}{P^6 Q^2} : \quad (C.13)$$

Consider the first term above, which we will denote by  $I$ . Integration over  $p$  gives a factor  $1/(8\pi p_0)$ , which follows from (B.3). The sum over  $p_0$  can be found by differentiation of (C.9):

$$\begin{aligned} p_0 \int_0^\infty e^{2ip_0 \cdot r} &= \frac{1}{2} \frac{d}{dr} e^{2ip_0 \cdot r} \\ &= T \cosh^2 r : \end{aligned} \quad (C.14)$$

This yields

$$I = \frac{T^2}{4(4\pi)^2} \int_0^\infty \frac{dr}{r} \coth r - 1 = r \int_{r=3r}^i \cosh^2 r : \quad (C.15)$$

The integral  $I$  which we have obtained is convergent, so one may evaluate it numerically. However, it is divergent term by term. Arnold and Zhai [11] have invented a regularization technique to compute these terms.

The first integral needed is

$$\int_0^\infty \frac{dr}{r} r^z : \quad (C.16)$$



Depending on the value of  $z$ , the contribution to the integral from one of the limits vanishes (and the other blows up). Thus, if one analytically continues  $z$  independently to regulate the behaviour at  $r = 0$  and  $r = 1$ , the integral in (C.16) vanishes.

We also have the result

$$\int_0^1 dr r^z e^{ar} = a^{-1-z} (1+z); \quad (C.17)$$

for the values of  $z$  for which the integral is well defined. The integral is then defined for all values of  $z$  by analytic continuation. This makes it possible to attack integrals of hyperbolic functions times powers of  $r$ :

$$\begin{aligned} \int_0^1 dr r^z \coth r &= \int_0^1 dr r^z \left( 1 + \sum_{n=1}^{\infty} e^{-2nr} \right) \\ &= 2^{-z} (1+z) (1+z); \end{aligned}$$

In the last line, we have used the definition of the Riemann zeta function as well as (C.17).

More complicated integrals, such as products between  $\operatorname{csch} r$  and  $\coth r$  can be computed from the above formulas using integration by parts:

$$\int_0^1 dr \coth r \operatorname{csch} r = \frac{z(z-1)}{2} \int_0^1 dr \frac{1}{r^2} = \frac{z(z-1)}{2}; \quad z \neq 0; \quad (C.18)$$

$$\int_0^1 dr \operatorname{csch} r = \frac{z}{2} \int_0^1 \frac{1}{r^2} = \frac{z}{2}; \quad z \neq 2; \quad (C.19)$$

$$\int_0^1 dr \operatorname{csch} r r^3 = \frac{1}{3} \int_0^1 \frac{1}{r^2} = \frac{1}{3}; \quad z \neq 1; \quad (C.20)$$

Employing the series expansions of the Gamma and Riemann Zeta functions we immediately get

$$I = \frac{1}{(4\pi)^2} \frac{T^{2h}}{24} \left( 3 + 2\epsilon + 2 \frac{\Gamma(1)}{\Gamma(1)} \right); \quad (C.21)$$

Finally, there is the second term in C.13. From Appendix A, one gets

$$\frac{1}{(4\pi)^2} \frac{T^{2h}}{24} + 4 \ln \frac{1}{4T} + 2\epsilon + 4 + 2 \frac{\Gamma(1)}{\Gamma(1)}; \quad (C.22)$$

Adding up (C.6), (C.13) and (C.22) we obtain (A.9).

Let us finally calculate the three dimensional one-loop diagram (B.3)

$$J = \int \frac{1}{p^2 + m^2}; \quad (C.23)$$

This can be obtained from the Fourier transform of the propagator in momentum space, which in three dimensions simply is the Yukawa potential:

$$\begin{aligned} V(R) &= \int \frac{d^3p}{(2\pi)^3} \frac{1}{p^2 + m^2} e^{ip \cdot R} \\ &= \frac{e^{-mR}}{4\pi R} = \frac{1}{4\pi R} K_0(mR) \end{aligned} \quad (C 24)$$

Here,  $K_0(x)$  is a modified Bessel function. Differentiation of (C 24) with respect to  $m$  and evaluating the expression at  $R = 0$  yields the desired result for  $J_0$ , (B 3).

## References

- [1] L. Dolan and R. Jackiw, Phys. Rev. D 9, 3320, 1974.
- [2] E. Braaten and R. Pisarski, Nucl. Phys. B 337, 569, 1990.
- [3] M. Le Bellac, Thermal Field Theory, Cambridge University Press, Cambridge 1996.
- [4] P. Arnold and O. Espinosa, Phys. Rev. D 47, 3546, 1993.
- [5] A. Hebecker, Z. Phys. C 60, 271, 1993.
- [6] Z. Fodor and A. Hebecker, Nucl. Phys. B 432, 127, 1994.
- [7] J. Frenkel, A. V. Saa and J. C. Taylor, Phys. Rev. D 46, 3670, 1992.
- [8] R. Parwani, Phys. Rev. D 51, 4518, 1995.
- [9] C. Coriano and R. Parwani, Nucl. Phys. B 434, 56-84, 1995.
- [10] R. Parwani, Phys. Lett. B 334, 420, 1994, ERRATUM ~~ibid.~~ B 342, 454, 1995.
- [11] P. Arnold and C. Zhai, Phys. Rev. D 50, 7603, 1994; Phys. Rev. D 51, 1906, 1995.
- [12] C. Zhai, B. Kastening, Phys. Rev. D 52, 7232, 1995.
- [13] G. P. Lepage, in From actions to answers, proceedings of the Advanced Study Institute in Elementary Particle Physics, Boulder, Colorado, 1989, edited by T. DeGrand and D. Toussaint, World Scientific, 1989.
- [14] N. P. Landsman, Nucl. Phys. B 322, 498, 1989.
- [15] D. J. Gross, R. D. Pisarski and L. G. Yaer, Rev. Mod. Phys. 53, 43, 1981.

- [16] E. Braaten and A. Nieto, Phys. Rev. D 53, 3421, 1996.
- [17] E. Braaten and A. Nieto, Phys. Rev. D 51, 6990, 1995.
- [18] J. O. Andersen, Phys. Rev. D 53, 7286, 1996.
- [19] A. Jakovac, A. Patkos, P. Petreczky, Phys. Lett. B 367, 283, 1996.
- [20] K. Farakos, K. Kajantie, K. Rummukainen, M. Shaposhnikov. Nucl. Phys. B 425, 67, 1994.
- [21] K. Kajantie, M. Laine, K. Rummukainen, M. Shaposhnikov, Nucl. Phys. B 458, 90, 1996.
- [22] D. Bodeker, P. John, M. Laine, and M. G. Schmidt, Nucl. Phys. B 497, 387, 1997.
- [23] A. D. Linde, Rep. Prog. Phys. 42, 389, 1979.
- [24] P. Arnold and L. G. Ya e, Phys. Rev. D 49, 3003, 1994.
- [25] I. Lawrie, Nucl. Phys. B 200, 1, 1982.
- [26] T. Appelquist and Carrazzone, Phys. Rev. D 11, 2856, 1975.
- [27] P. Ginsparg, Nucl. Phys. B 170, 388, 1980.
- [28] A. Jakovac, Phys. Rev. D 53, 4538, 1996.
- [29] J. O. Andersen, Z. Phys. C 75, 147, 1997; Ph.D. thesis, University of Oslo, 1997.
- [30] L. H. Ryder, Quantum Field Theory, Cambridge University Press, Cambridge, 1985.
- [31] J. I. Kapusta, Finite Temperature Field Theory, Cambridge University Press, Cambridge, 1989.

FIGURE CAPTIONS:

Figure 1: The tadpole in scalar theory.

Figure 2: One-loop scalar self-energy diagrams in the full theory.

Figure 3: One-loop diagrams for the photon polarization tensor in the full theory.

Figure 4: Two-loop scalar self-energy diagrams in SQED.

Figure 5: Two-loop self-energy diagrams for the timelike component of the gauge field in SQED.

Figure 6: One-loop graphs contributing to the scalar four-point function in the full theory.

Figure 7: One-loop diagrams needed for calculating the couplings  $e_E^2(\mu)$  and  $h_E^2(\mu)$ .

Figure 8: One-loop diagrams contributing to the four-point function of  $\phi$  in SQED.

Figure 9: One and two-loop diagrams contributing to the scalar self-energy function in ESQED.

Figure 10: One-loop diagram relevant for the calculation of scalar self-coupling in ESQED.

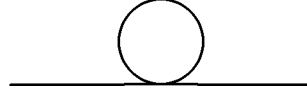


Figure 1: The tadpole in scalar theory.



Figure 2: One-loop scalar self-energy diagrams in the full theory.

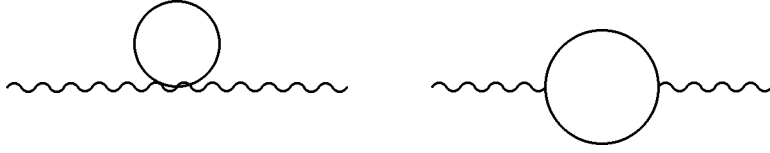


Figure 3: One-loop diagrams for the photon polarization tensor in the full theory.

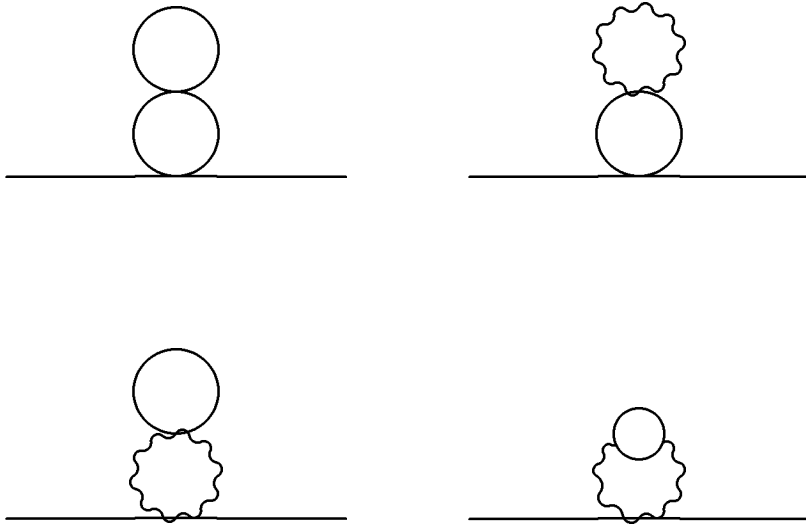


Figure 4: Two-loop scalar self-energy diagrams in SQED.

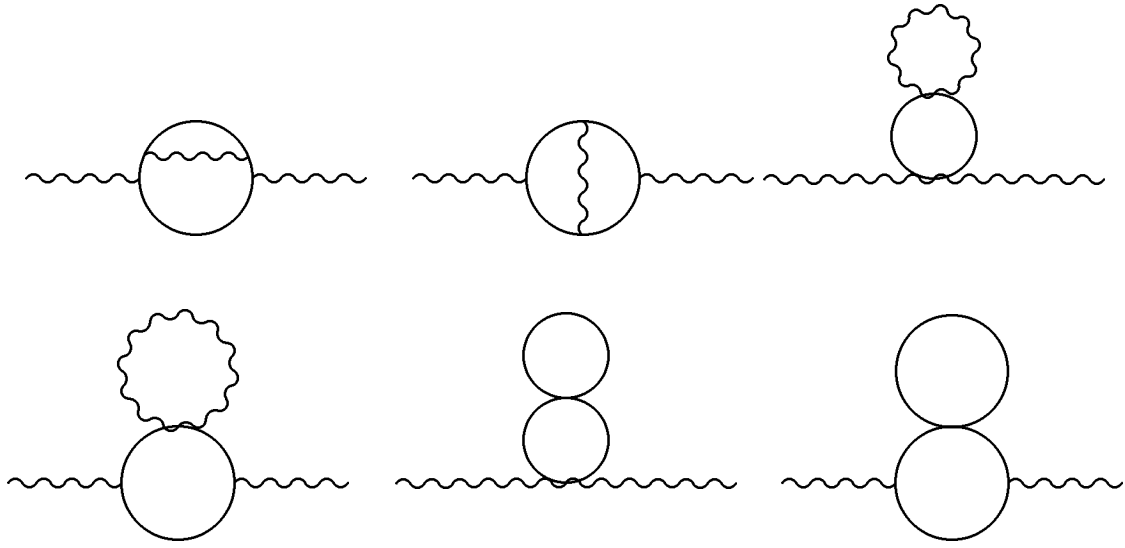


Figure 5: Two-loop self-energy diagrams for the timelike component of the gauge field in SQED.



Figure 6: One-loop graphs contributing to the scalar four-point function in the full theory.

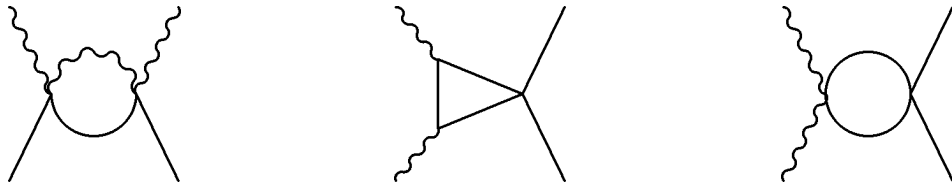


Figure 7: One-loop diagrams needed for the calculating the couplings  $e_E^2$  and  $h_E^2$ .

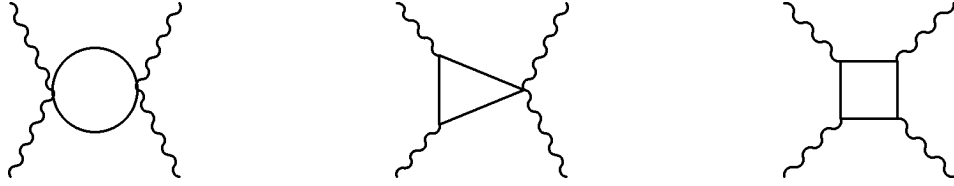


Figure 8: One-loop diagrams contributing to the four-point function of in SQED .

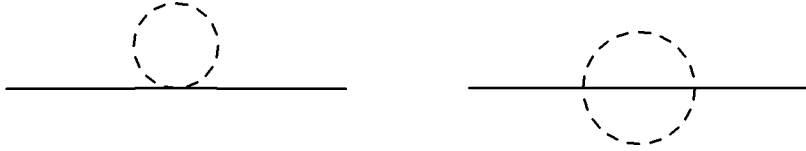


Figure 9: One and two-loops diagram contributing to the scalar selfenergy function in ESQED .

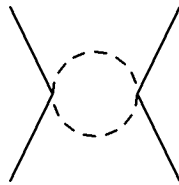


Figure 10: One-loop diagram relevant for the calculation of scalar self-coupling in ESQED .